Thermonuclear reaction rate of ^{18}Ne(α,p)^{21}Na from Monte Carlo calculations

P. Mohr, R. Longland, and C. Iliadis

Thermonuclear reaction rate of ^{18}Ne(α,p)^{21}Na from Monte-Carlo calculations

P. Mohr,[1, 2, *] R. Longland,[3, 4] and C. Iliadis[3, 4]

[1]*Diakonie-Klinikum, D-74523 Schwäbisch Hall, Germany*
[2]*Institute for Nuclear Research (ATOMKI), H-4001 Debrecen, Hungary*
[3]*Department of Physics and Astronomy, University of North Carolina, Chapel Hill, NC 27599-3255, USA*
[4]*Triangle Universities Nuclear Laboratory, Durham, NC 27708-0308, USA*
(Dated: November 28, 2014)

The ^{18}Ne(α,p)^{21}Na reaction impacts the break-out from the hot CNO-cycles to the *rp*-process in type I X-ray bursts. We present a revised thermonuclear reaction rate, which is based on the latest experimental data. The new rate is derived from Monte-Carlo calculations, taking into account the uncertainties of all nuclear physics input quantities. In addition, we present the reaction rate uncertainty and probability density versus temperature. Our results are also consistent with estimates obtained using different indirect approaches.

PACS numbers: 25.60.-t,25.55.-e,26.30.-k

I. INTRODUCTION

There has been much interest recently in the thermonuclear rate of the ^{18}Ne(α,p)^{21}Na reaction at temperatures of type I X-ray bursts [1, 2]. Because of the high temperatures of several Giga-Kelvin (in usual notation: $T_9 \approx 1 - 2$), the reaction rate is essentially defined by the cross section at energies between 1 and 3 MeV. This corresponds to excitation energies of $E^* \approx 9 - 11$ MeV in the compound nucleus ^{22}Mg.

The latest studies have focused on indirect determinations of the ^{18}Ne(α,p)^{21}Na reaction rate. Matic *et al.* [3] obtained excitation energies, E^*, of many levels in the ^{22}Mg compound nucleus by measuring the ^{24}Mg(p,t)^{22}Mg reaction. These energies define the resonance energies, E, in the ^{18}Ne(α,p)^{21}Na reaction, which enter exponentially into the expression for the reaction rate and are thus the most important ingredient. From the same experiment, total widths Γ of these states were derived [4]. In addition, spins and parities, J^π, of several states in ^{22}Mg have been measured recently by resonant proton scattering using the ^{21}Na(p,p)^{21}Na reaction in inverse kinematics [5, 6]. Furthermore, the reverse ^{21}Na(p,α)^{18}Ne reaction has been used in two independent experiments [7, 8] to determine a lower limit of the forward ^{18}Ne(α,p)^{21}Na reaction cross section. Mohr and Matic [4] found a dramatic disagreement between the earlier forward ^{18}Ne(α,p)^{21}Na reaction data obtained by Groombridge *et al.* [9] and the reverse reaction data [7, 8]. Consequently, the data of Ref. [9] were excluded from the determination of the reaction rate in Ref. [4].

Two different approaches have been used in Ref. [4] to determine the ^{18}Ne(α,p)^{21}Na reaction rate from the available data. In the first approach, the experimental resonance energies from the ^{24}Mg(p,t)^{22}Mg reaction [3], together with α-transfer data for the mirror compound nucleus ^{22}Ne [3], were employed for calculating the required resonance strengths, $\omega\gamma_{\alpha p}$. In the second approach, the experimental reverse reaction data [7, 8] were corrected for thermal target excitations by using a Hauser-Feshbach model and the forward rate was obtained using the reciprocity theorem. It was shown in Ref. [4] that the reaction rates obtained by these two methods differ by a factor of ≈ 3. Taking into account estimated uncertainties of a factor of ≈ 2 for both approaches, the geometric mean value has been recommended in Ref. [4].

The present study involves several major improvements compared to the procedure of Ref. [4]. We employ the latest J^π assignments from resonant ^{21}Na(p,p)^{21}Na elastic scattering [5, 6]. Furthermore, for all states seen in the ^{24}Mg(p,t)^{22}Mg transfer experiment [3], improved resonance strengths, $\omega\gamma_{\alpha p}$, are determined (Sec. III). The new resonance strengths are used as input for a Monte-Carlo sampling method [10–13], which provides for the first time the rate probability densities of the ^{18}Ne(α,p)^{21}Na reaction. From these results we extract statistically meaningful thermonuclear rates and rate uncertainties (Sec. IV). Finally, the break-out temperature and its uncertainty are given for typical conditions of type I X-ray bursts.

II. PRELIMINARY CONSIDERATIONS

The reaction rate, $N_A\langle\sigma v\rangle$, of the ^{18}Ne($\alpha$,$p$)^{21}Na reaction is given by the sum over the contributions of many resonances. (Strictly speaking, the reaction rate is obtained after multiplying $N_A\langle\sigma v\rangle$ with the densities of the reaction partners and integration over space. Nevertheless, the quantity $N_A\langle\sigma v\rangle$ is usually called "reaction rate". We keep this convention throughout this paper.)

A simplified level scheme for the ^{18}Ne(α,p)^{21}Na reaction is shown in Fig. 1 for illustration purposes. Because of the positive Q-value of this reaction, the available energy in the ^{21}Na+p channel is much higher than in the ^{18}Ne+α channel. Simultaneously, the Coulomb barrier is much lower in the ^{21}Na+p channel ($Z_1 \times Z_2 = 11$) com-

pared to the ^{18}Ne+α channel ($Z_1 \times Z_2 = 20$). Hence, the proton partial width is much larger compared to the α-particle partial width for all relevant resonances, $\Gamma_p \gg \Gamma_\alpha$, and the γ-ray partial width, Γ_γ, is very small compared to the total width, $\Gamma_p \approx \Gamma$.
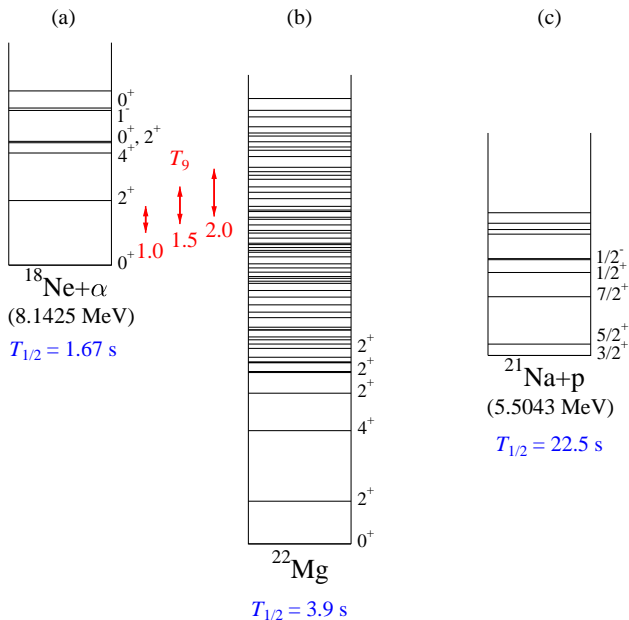

FIG. 1. (Color online) Level scheme of the compound nucleus ^{22}Mg (b) with the ^{18}Ne+α (a) and ^{21}Na+p (c) thresholds (approximately to scale). The energies are given in MeV. The energy range of the classical Gamow window is indicated for three temperatures, $T_9 = 1.0$, 1.5, and 2.0 by red arrows.

It has been shown in Ref. [4] that the reaction rate can be calculated using the narrow resonance formalism [14]:

$$N_A \langle \sigma v \rangle = \frac{1.54 \times 10^{11}}{(\mu T_9)^{3/2}} \sum_i \frac{(\omega\gamma_{\alpha p})_i}{e^{11.605 E_i/T_9}} \; \text{cm}^3\,\text{s}^{-1}\,\text{mol}^{-1} \tag{1}$$

with the reduced mass, μ, in units of amu, the resonance energies, E_i, in MeV, and the resonance strengths, $(\omega\gamma_{\alpha p})_i$, in MeV. In this work, resonance energies and excitation energies are denoted by E and E^*, respectively. All quantities are given in the center-of-mass (c.m.) system unless noted otherwise. The deviations between the simple narrow-resonance formalism and a numerical integration of the cross section $\sigma(E)$ in $N_A \langle \sigma v \rangle$ remain below $5\,\%$ for $T_9 = 1-2$ and below $10\,\%$ for a wider temperature range of $T_9 = 0.25 - 3$ [4].

Resonance energies are derived from the measured excitation energies [3] by using $E = E^* - S_\alpha$, with the α-particle binding energy in the ^{22}Mg compound nucleus given by $S_\alpha = 8142.5 \pm 0.5$ keV [15]. The uncertainty of S_α does not significantly affect the uncertainty of the reaction rate. The resonance energies are thus well constrained by the high-resolution transfer experiment of Ref. [3]. Earlier transfer experiments [16–19] show good agreement with the high-resolution data [3] (for a de-

tailed discussion, see Ref. [4]).

The resonance strength, $\omega\gamma_{\alpha p}$, for a resonance with spin J in the ^{18}Ne(α,p)^{21}Na reaction is given by

$$\omega\gamma_{\alpha p} = (2J + 1)\frac{\Gamma_\alpha \Gamma_p}{\Gamma} \approx (2J + 1)\Gamma_\alpha \tag{2}$$

where the approximations $\Gamma_p \approx \Gamma$ and $\Gamma_\alpha \ll \Gamma_p$ are used in Eq. (2). Thus, the essential quantity defining the resonance strength is the partial width Γ_α for the decay of an excited level into the ^{18}Ne+α channel. The estimation of Γ_α for ^{22}Mg levels from properties of the mirror states in ^{22}Ne will be described in detail in Sec. III.

The first excited state in ^{18}Ne with $J^\pi = 2^+$ is located at a relatively high excitation energy of $E^* = 1887$ keV. In a stellar plasma the population of the first excited state remains negligible with $(2J + 1)\exp(-E^*/kT) \lesssim 10^{-4}$ up to temperatures $T_9 < 2$, and the contributions of higher-lying states are even smaller. Thus, at typical temperatures of type I X-ray bursts the *stellar* rate of the ^{18}Ne(α,p)^{21}Na reaction (i.e., including thermal target excitations) is practically identical to the *laboratory* rate (i.e., for target ground state population only).

The situation is different for the reverse ^{21}Na(α,p)^{18}Ne reaction. Low-lying states in ^{21}Na may be populated under stellar conditions, and a laboratory measurement of the ^{21}Na(p,α)^{18}Ne reaction cannot determine the stellar ^{21}Na(p,α)^{18}Ne rate. The laboratory measurement provides only the partial ^{21}Na$_{\text{g.s.}}$(p,α)^{18}Ne$_{\text{g.s.}}$ cross section. This statement holds exactly for low proton energies below 4.5 MeV where the reaction channel to the first excited state in ^{18}Ne is closed. But also at slightly higher energies this statement holds approximately because the Coulomb barrier strongly prefers the ground state channel, and no event for the first excited state has been detected in the experiment of Salter *et al.* [7].

From the above considerations we may conclude that a measurement of the reverse ^{21}Na(p,α)^{18}Ne reaction only provides the ^{18}Ne$_{\text{g.s.}}$(α,p)^{21}Na$_{\text{g.s.}}$ cross section using the reciprocity theorem of nuclear reactions. A reaction rate which is determined from this ground state to ground state cross section is only a lower limit for the stellar rate of the forward ^{18}Ne(α,p)^{21}Na reaction which populates the ground state and low-lying states of ^{21}Na.

For completeness we mention that *stellar* reaction rates of forward and reverse reactions are directly related by detailed balance. However, this general relation does not hold for rates which are determined from laboratory cross sections.

The thermonuclear rate of the ^{18}Ne(α,p)^{21}Na reaction covers many orders of magnitude in the relavant temperature range. Therefore, it is helpful to compare the present results to a reference rate. For the latter we adopt the rate of Ref. [4], which is based on experimental resonance energies and total widths and on calculated α-particle partial widths and resonance strengths (see Tables I and II of Ref. [4]).

III. DETERMINATION OF RESONANCE STRENGTHS

The partial widths Γ_α of ^{22}Mg levels in the relevant energy window have not been measured directly yet. Hence indirect methods have to be applied to determine Γ_α. In such cases, the assumption of mirror symmetry in the wave functions of corresponding ^{22}Mg and ^{22}Ne levels yields for the dimensionless reduced widths

$$\theta_\alpha^2(^{22}\text{Mg}) \approx \theta_\alpha^2(^{22}\text{Ne}) \qquad (3)$$

Equation (3) is typically fulfilled for states with a strong α-cluster component in the wave function (i.e., for a large value of θ_α^2), whereas significant discrepancies have been found for mirror states with very small θ_α^2 values [20].

Here we follow the procedure for estimating Γ_α in ^{22}Mg that was outlined in Ref. [3], but implement several improvements. We group the astrophysically important ^{22}Mg levels, listed in Refs. [3, 4] into four different categories, which will be discussed below in more detail.

A. Resonance strengths from reduced widths in the ^{22}Ne mirror nucleus

Category A represents states with known Γ_α in the mirror nucleus ^{22}Ne. Absolute Γ_α values can be determined from ^{18}O(α,γ)^{22}Ne reaction data for a few low-lying resonances [21–24] and from resonant ^{18}O(α,α)^{18}O elastic scattering at higher energies [25]. However, the latter do not play a significant role in the determination of $N_A\langle\sigma v\rangle$ because of the relatively high energies. For states in this category A, we assign an uncertainty of a factor of two to the derived partial widths, Γ_α, in ^{22}Mg. The corresponding Γ_α values in ^{22}Ne are typically known with much smaller uncertainties. The factor of two uncertainty reflects the assumption of mirror symmetry of the wave functions in Eq. (3).

Category B consists of a few high-lying states, corresponding to resonance energies above 3.5 MeV, with known Γ_α values in the ^{22}Ne mirror nucleus from resonant ^{18}O(α,α)^{18}O elastic scattering [25]. Because of their high resonance energy, the partial widths Γ_α in ^{22}Mg become very large, and the approximation $\Gamma_\alpha \ll \Gamma$ does not hold anymore. In this case the resonance strengths, $\omega\gamma_{\alpha p} = \omega\Gamma_\alpha\Gamma_p/\Gamma$, are determined using $\Gamma_p = \Gamma - \Gamma_\alpha$ where the total widths Γ are taken from [4] and the partial widths Γ_α are calculated from Eq. (3) and θ_α^2 from [25]. For states in this category we assign a resonance strength uncertainty of a factor 3. Note that these levels have practically no impact on $N_A\langle\sigma v\rangle$ at astrophysically relevant temperatures.

Category C is assigned to states with known spectroscopic information from α-transfer on ^{18}O. The relevant excitation energy range was studied in Ref. [23] using the ^{18}O(^{6}Li,d)^{22}Ne reaction at $E_{\text{lab}} = 32$ MeV. Because only relative spectroscopic factors are reported in Ref. [23], an

absolute normalization of the transfer data has to be performed (see below). For states in this category, we assign a resonance strength uncertainty of a factor 3, which is a combined uncertainty of the assumption of mirror symmetry in Eq. (3) and the model dependence introduced by deriving Γ_α from α-transfer. The estimate of a factor of two uncertainty for the assumption of mirror symmetry was already explained for the Category A states above. We estimate another factor of two uncertainty for the model dependence of the determination of reduced widths θ_α^2 and absolute partial widths Γ_α from transfer. Combining both uncertainty factors using quadratic error propagation for lognormal distributions, leads to an overall uncertainty factor of $\sqrt{2^2 + 2^2} = \sqrt{8} \approx 3$.

Category D is assigned to all of the remaining levels for which no spectroscopic information is available. As a crude estimate, Matic *et al.* [3] adopted for these states a reduced width that was obtained by averaging the experimental values of levels observed in transfer studies. This procedure is problematic because transfer reactions preferentially populate states with large reduced widths, θ_α^2. In other words, states that have not been observed in transfer reactions presumably have smaller reduced widths compared to the average of the detected states. Therefore, the procedure applied by Ref. [3] significantly overestimates the actual dimensionless reduced width, θ_α^2, and thus the α-particle partial width, Γ_α. In this work, we randomly sample θ_α^2 for all states in Category D from a Porter-Thomas distribution with a mean reduced width of $\langle\theta_\alpha^2\rangle = 0.03 \pm 0.01$. We obtain this value by extrapolating the recent results of Pogrebnyak *et al.* [26] for nuclei with slightly larger mass numbers A. In the latter work, $\langle\theta_\alpha^2\rangle = 0.018$ was found with a trend to increasing values for smaller mass numbers. The value of $\langle\theta_\alpha^2\rangle = 0.03 \pm 0.01$ used in the present work leads to a significantly reduced reaction rate compared to the results of Ref. [3], as shown below. We also find that the uncertainty in this value has only a minor impact on the total rate. A further uncertainty for $N_A\langle\sigma v\rangle$ arises from only tentative J^π assignments for these category D states without detailed spectroscopic information. This will be discussed later (see Sect. IV).

The partial width Γ_α is calculated from the single-particle (*s.p.*) limit according to

$$\Gamma_\alpha = \theta_\alpha^2 \times \Gamma_\alpha^{s.p.} \qquad (4)$$

where $\Gamma_\alpha^{s.p.}$ is computed using a radius of $R = R_0 \times (A_P^{1/3} + A_T^{1/3})$, with $R_0 = 1.25$ fm. This value of the radius parameter is chosen for consistency with Ref. [26]. The choice of R_0 has only a small influence on the calculated Γ_α values in ^{22}Mg because the same R_0 has been used in the determination of $\theta_\alpha^2(^{22}\text{Ne})$ from $\Gamma_\alpha(^{22}\text{Ne})$ and in the determination of $\Gamma_\alpha(^{22}\text{Mg})$ from $\theta_\alpha^2(^{22}\text{Mg}) \approx \theta_\alpha^2(^{22}\text{Ne})$.

Apart from the above modification in the treatment of states without spectroscopic information (category D), we implement two other improvements compared to earlier work [3, 4].

First, for some states very small reduced widths, on the order of 10^{-5}, were reported in Ref. [3], which were derived from $^{18}O(\alpha,\gamma)^{22}Ne$ capture data [21]. However, for these resonances the neutron channel is also open, and it is not possible to derive Γ_α from the measured (α,γ) resonance strength, $\omega\gamma_{\alpha\gamma} = (2J+1)\Gamma_\alpha\Gamma_\gamma/\Gamma \neq (2J+1)\Gamma_\alpha$, because the total width, Γ, may be dominated by the neutron width, Γ_n. We have assigned these states either to category C or category D, depending on whether reduced widths were measured in the transfer experiment [23].

Second, as already pointed out above, only relative spectroscopic factors are available for the states assigned to category C. Matic *et al.* [3] normalized the transfer data to theoretical spectroscopic factors, either of the ground state or of the state at $E^* = 10066$ keV. In the present work we instead normalize the spectroscopic factors to experimental values only. The 1^- state in the ^{22}Ne mirror nucleus at $E^* = 10209$ keV has been detected in the $^{18}O(^6Li,d)^{22}Ne$ transfer experiment [23] and in several $^{18}O(\alpha,\gamma)^{22}Ne$ capture experiments [21–23]. The capture results are in excellent agreement. The most recent capture experiment [24] recommends an experimental resonance strength of $\omega\gamma_{\alpha\gamma} = 229 \pm 19\,\mu eV$, which was also used to determine the strengths of lower-lying observed resonances. From this experimental value, an α-particle partial width and a reduced width of $\Gamma_\alpha = \omega\gamma/3 = 76.3\,\mu eV$ and $\theta_\alpha^2 = 0.150 \pm 0.012$, respectively, can be derived using $R_0 = 1.25$ fm. Giesen *et al.* [23] report for this level, which is located below the neutron threshold in ^{22}Ne, a relative spectroscopic factor of $S_{rel} = 0.035$ from an $^{18}O(^6Li,d)^{22}Ne$ experiment. Consequently, we scaled all relative spectroscopic factors of Ref. [23] by a factor $f = 0.150/0.035 = 4.29$ in order to obtain the reduced width, θ_α^2. Although the uncertainty in f is small, we assigned a factor of 3 uncertainty to all resonance strengths of category C levels that involved an estimate of Γ_α in ^{22}Mg using this scaling factor.

Our recommended resonance strengths, $\omega\gamma_{\alpha p}$, are listed in Table I. For states in category D we provide $\omega\gamma$ in parenthesis which are calculated from $\Gamma_\alpha = 0.03 \times \Gamma_\alpha^{s.p.}$ where the factor of 0.03 is taken from the systematics of reduced widths [26]. Note that these resonance strengths are used in the presentation of the recommended astrophysical S-factor in the next paragraph; however, these numbers do not enter directly in the calculation of $N_A\langle\sigma v\rangle$ because here a Porter-Thomas distribution will be sampled using the Monte-Carlo method. Additionally, the previous values, $\omega\gamma_{ref}$, from Tables I and II of Ref. [4] are provided for comparison.

The astrophysical S-factor, $S(E)$, of the $^{18}Ne(\alpha,p)^{21}Na$ reaction, calculated using the present resonance strengths that are listed in Tab. I, is displayed in Fig. 2. The total widths, Γ, are also adopted from experimental data (Ref. [4] and Tab. I). For states in category D where reduced widths θ_α^2 are unknown the numbers in parenthesis in Table I were used. The present S-factor is slightly smaller than the result of Ref. [4] in the energy region

$1300\,keV \lesssim E \lesssim 2200\,keV$, and is significantly smaller at lower and higher energies. Our smaller S-factor at very low energies results partly from the new spin assignments and partly from the smaller reduced widths, θ_α^2, and resonance strengths, $\omega\gamma_{\alpha p}$, for the category D resonances. The smaller S-factor at higher energies, around 2500 keV, results mainly from the new spin assignments of category D levels. Notice in the figure the broad peak resulting from the 0^+ resonance at 1567 keV, which will strongly contribute to the reaction rate (Sec. III B). A similar statement holds for the 1^- resonance at 938 keV, which impacts the reaction rate at temperatures slightly below $T_9 = 1$.

The Hauser-Feshbach model calculation (dash-dotted green line) is not able to reproduce the individual resonances in the $^{18}Ne(\alpha,p)^{21}Na$ S-factor. Nevertheless, the general trend of the energy dependence is approximately reproduced. Thus, it can be expected that the statistical model is able to provide the correct order of magnitude for the reaction rate $N_A\langle\sigma v\rangle$. As already discussed in Sec. II, the experimental cross section of the reverse $^{21}Na(p,\alpha)^{18}Ne$ reaction can be used to derive the ground state contribution of the $^{18}Ne_{g.s.}(\alpha,p)^{21}Na_{g.s.}$ cross section. Both available data sets (6 data points in [7] and 2 data points and 3 upper limits in [8]) are in reasonable agreement with each other. As expected, the experimental ground state contribution is lower than the present total S-factor.
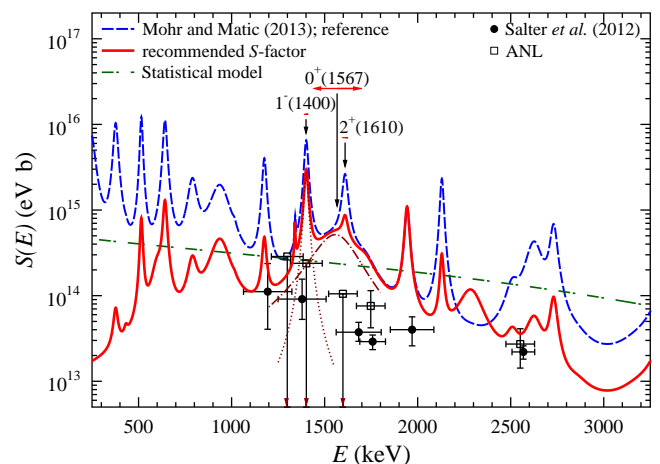
FIG. 2. (Color online) Astrophysical S-factor of the $^{18}Ne(\alpha,p)^{21}Na$ reaction versus center-of-mass energy E, calculated from the resonance properties listed in Tab. I (thick red line). For comparison: (dashed blue line) Ref. [4], so-called reference (for details see [4]); (dash-dotted green line) Hauser-Feshbach statistical model, taken from [33]. The experimental data points shown are derived from the reverse $^{21}Na(p,\alpha)^{18}Ne$ reaction [7, 8] and represent the ground state contribution $^{18}Ne_{g.s.}(\alpha,p)^{21}Na_{g.s.}$ only. The contributions of the two resonances at 1400 keV and 1567 keV are shown with dashed and dash-dotted dark-red lines, respectively. The total widths, Γ, are indicated by horizontal dark-red arrows. See the text.

TABLE I. Properties of resonances in ^{18}Ne$(\alpha,p)^{21}$Na; the new resonance strengths $\omega\gamma_{\alpha p}$ from this work are compared to the reference strengths $\omega\gamma_{\mathrm{ref}}$ from Ref. [4]. Excitation energies in the compound nucleus ^{22}Mg and the mirror assignments in ^{22}Ne are given. All reference values are adopted from Ref. [4]. Dimensionless reduced widths labeled "PT" indicate states of category D; for the calculation of the reaction rate Γ_α is sampled according to a Porter-Thomas distribution with $\langle\theta_\alpha^2\rangle = 0.03 \pm 0.01$ (see the text for details). For these states we provide $\omega\gamma_{\alpha p} \approx (2J+1)\Gamma_\alpha = (2J+1) \times 0.03 \times \Gamma_\alpha^{s.p.}$ in parenthesis.

$E^*(^{22}$Mg$)$ (MeV)	E (MeV)	J^π_{ref}	Γ_{ref} (keV)	$\omega\gamma_{\mathrm{ref}}$ (eV)	J^π	$\omega\gamma$ (eV)	θ_α^2	category	$E^*(^{22}$Ne$)$ (MeV)
8.182	0.040	[2$^+$]	33.5±2.2	8.53×10^{-65}	2$^+$ [a]	(3.30×10^{-66})	PT	D	8.489
8.385	0.243	[2$^+$]	47.0±5.3	1.33×10^{-17}	1$^+$ [b]	–	–	–	
8.519	0.377	[2$^+$]	25.7±4.1	1.53×10^{-11}	3$^-$ [c]	7.05×10^{-14}	0.017	C	8.740
8.574	0.432	[4$^+$]	20.6±16.8	3.26×10^{-12}	4$^+$ [d]	(5.05×10^{-13})	PT	D	8.855
8.657	0.515	[0$^+$]	15.5±3.5	4.97×10^{-8}	2$^+$ [e]	(3.13×10^{-9})	PT	D	8.596
8.743	0.601	[4$^+$]	65.5±22.8	5.15×10^{-9}	2$^+$ [f]	(1.23×10^{-7})	PT	D	9.045
8.783	0.641	[1$^-$]	22.5±7.0	1.21×10^{-5}	1$^-$ [g]	(1.32×10^{-6})	PT	D	9.097
8.932	0.790	[2$^+$]	51.6±5.9	4.13×10^{-4}	2$^+$ [h]	(4.14×10^{-5})	PT	D	9.229
9.080	0.938	[1$^-$]	114.4±19.7	2.31×10^{-2}	1$^-$ [i]	5.25×10^{-3}	0.064	C	9.324
9.157	1.015	[4$^+$]	< 20.5	8.70×10^{-4}	4$^+$ [j]	(1.01×10^{-4})	PT	D	9.508
9.318	1.176	[2$^+$]	22.6±8.0	4.97×10^{-1}	2$^+$	(4.97×10^{-2})	PT	D	9.625
9.482	1.340	[3$^-$]	< 6.3	1.25×10^{-1}	3$^-$	1.35×10^{-1}	0.047	C	9.725
9.542	1.400	[1$^-$]	< 22.9	1.31×10^{1}	1$^-$	5.74×10^{0}	0.115	C	9.842
9.709	1.567	[0$^+$]	267.8±48.2	5.18×10^{1}	0$^+$	6.50×10^{1}	0.458	A	10.052
9.752	1.610	[1$^-$]	31.4±6.8	4.82×10^{1}	2$^+$ [k]	8.45×10^{0}	0.052	A	10.137
9.860	1.718	[0$^+$]	121.3±10.4	2.07×10^{1}	0$^+$	1.92×10^{1}	0.042	A	10.283
10.085	1.943	[2$^+$]	25.8±9.3	2.25×10^{2}	2$^+$	2.34×10^{2}	0.134	A	10.297
10.272	2.130	2$^+$	20.7±2.7	1.31×10^{3}	2$^+$	(1.49×10^{2})	PT	D	10.551
10.429	2.287	[4$^+$]	144.2±25.8	4.89×10^{1}	1$^-$ [l]	9.39×10^{2}	0.150	A	10.209
10.651	2.509	[3$^-$]	72.8±19.1	1.12×10^{3}	3$^-$	(2.65×10^{2})	PT	D	10.857
10.768	2.626	[2$^+$]	94.9±29.6	1.16×10^{4}	2$^+$	(1.29×10^{3})	PT	D	11.064
10.873	2.731	[0$^+$]	40.2±12.0	1.19×10^{4}	0$^+$	(1.59×10^{3})	PT	D	11.194
11.001	2.859	[4$^+$]	135.8±12.9	5.81×10^{2}	4$^+$	(2.13×10^{2})	PT	D	11.271
11.315	3.173	[4$^+$]	203.7±37.0	1.83×10^{3}	4$^+$	(6.21×10^{2})	PT	D	11.577
11.499	3.357	[2$^+$]	116.8±21.8	8.64×10^{4}	2$^+$	2.17×10^{4}	0.062	A	11.700 [m]
11.595	3.453	[4$^+$]	48.3±14.7	3.67×10^{3}	4$^+$	(1.41×10^{3})	PT	D	11.896
11.747	3.605	[0$^+$]	166.1±64.4	7.13×10^{4}	0$^+$	2.64×10^{4}	0.381	B	12.020 [m]
11.914	3.772	[2$^+$]	122.4±19.7	1.77×10^{5}	0$^+$	2.40×10^{4}	0.363	B	12.250 [m]
12.003	3.861	[1$^-$]	– [n]	4.31×10^{5}	1$^-$	3.84×10^{4}	0.354	A	12.280 [m]
12.185	4.043	[3$^-$]	236.4±52.0	2.60×10^{5}	2$^+$	9.50×10^{4}	0.077	A	12.390 [m]
12.474	4.332	[2$^+$]	193.8±51.6	3.89×10^{5}	2$^+$	6.96×10^{4}	0.039	A	12.610 [m]
12.665	4.523	[3$^-$]	128.8±23.5	3.45×10^{5}	3$^-$	6.56×10^{4}	0.050	A	12.890 [m]
13.010	4.868	[0$^+$]	600.9±114.5	2.16×10^{5}	0$^+$	5.63×10^{4}	0.047	A	12.990 [m]

[a] $J^\pi = 2^+$ confirmed in Ref. [6]
[b] new $J^\pi = 1^+$ assignment in Ref. [6]
[c] earlier $J^\pi = 3^-$ of [3] confirmed; $J^\pi = 2^+$ of Ref. [19] rejected in Ref. [6]
[d] $J^\pi = 4^+$ confirmed in Ref. [6]
[e] new $J^\pi = 2^+$ assignment in Ref. [6]
[f] new $J^\pi = 2^+$ assignment in Ref. [6]
[g] $J^\pi = 1^-$ confirmed in Ref. [6]
[h] $J^\pi = 2^+$ confirmed in Ref. [6]
[i] $J^\pi = 1^-$ confirmed in Ref. [6]
[j] $J^\pi = 4^+$ confirmed in Ref. [6]
[k] $J^\pi = 2^+$ from $J^\pi = (1^-, 2^+)$ in Ref. [19] and $J^\pi = (2^+, 3^-, 4^+)$ in Ref. [23]
[l] $J^\pi = 1^-$ from Ref. [19]
[m] E^*, J^π, and Γ_α adopted from Ref. [25]
[n] state adopted from Ref. [18]

B. The $E^* = 10066\,$keV level in ^{22}Ne

The level at $E^* = 10066\,$keV in ^{22}Ne, whose mirror in ^{22}Mg corresponds to a strong resonance at 1567 keV in the ^{18}Ne$(\alpha,p)^{21}$Na reaction, requires special attention. This state is tentatively assigned as $J^\pi = (0^+)$ in Ref. [27], but $J^\pi = 1^-$ or even 1^+ have also been suggested. In the present work we adopt $E^* = 10052\,$keV and $J^\pi = 0^+$, based on the following arguments.

First, the state must have natural parity because it has been observed in α-transfer [23] and α-capture [24] studies. In the electron scattering work of Ref. [28] it

is stated that "... two states (10.08 and 12.56 MeV) are compatible with either $J^\pi = 1^+$ or 1^-." However, a 2^+ assignment for the 10066 keV state was only excluded on purely theoretical grounds. A comparison of excitation energies from the electron scattering experiment [28] and the ENSDF database [27] shows an offset by about 50 keV for neighboring states, implying a corrected excitation energy of $E^* \approx 10.080\,\text{MeV} + 0.05\,\text{MeV} = 10.130\,\text{MeV}$. This value is in excellent agreement with the location of a $J^\pi = 2^+$ state at $E^* = 10.137\,\text{MeV}$ in ^{22}Ne [27]. Assuming an assignment of $J^\pi = 2^+$ results in a reduced transition strength of $B(E2)\downarrow = 8^{+1.6}_{-0.9}\,e^2\text{fm}^4$, which was excluded in Ref. [28] only because shell model calculations at that time predicted $B(E2)\downarrow \leq 3\,e^2\text{fm}^4$ (or $\leq 0.8\,\text{W.u.}$) However, modern calculations [30] result in larger transition strengths. Thus, it is likely that the 2^+ state at $E^* = 10137\,\text{keV}$ in ^{22}Ne has been detected by Ref. [28], and that the J^π assignment in Ref. [28] is incorrect.

A photon scattering experiment [29] did not observe any peak near $E^* = 10066\,\text{keV}$, consistent with a $J^\pi = 0^+$ assignment. In principle, the 2^+ state at $E^* = 10137\,\text{keV}$ could have been observed in the photon scattering experiment. However, the reduced transition strength measured in the electron scattering experiment [28] results in 2.2 W.u. for the ground state transition, which is most likely below the detection limit in the photon scattering measurement [29].

The $J^\pi = 0^+$ assignment for the state at 10066 keV is also preferred by $(^6\text{Li},d)$ transfer data [23], although $J^\pi = 1^-$ cannot be ruled out. Furthermore, several theoretical calculations predict a $J^\pi = 0^+$ state with a large α-particle reduced width, θ_α^2, near $E^* \approx 10\,\text{MeV}$ [30–32], consistent with the large reduced widths found both in α-capture and α-transfer.

Consequently, we assign here $J^\pi = 0^+$ to this level, and we adopt a slightly lower excitation energy of $E^* = 10052\,\text{keV}$, based on α-capture and α-transfer data [23, 24] and disregarding the value of $E^* = 10080\,\text{keV}$ from electron scattering [28].

The measured strength of the corresponding resonance in $^{18}\text{O}(\alpha,\gamma)^{22}\text{Ne}$ amounts to $\omega\gamma_{\alpha\gamma}^{exp} = 0.24 \pm 0.08\,\mu\text{eV}$ [24]. The uncertainty is relatively large and yields a value of $\theta_\alpha^2 = 0.27 \pm 0.09$ for the dimensionless reduced α-particle width. It should be noted that the α-capture experiment [24] applied a coincidence technique, where the resonance strength $\omega\gamma_{\alpha\gamma}^{exp}$ was derived using the measured yield of the $2^+ \to 0^+$ transition from the first excited state in ^{22}Ne to the ground state. This measured *partial* resonance strength has been increased by Ref. [24] to an estimated total strength of $\omega\gamma_{\alpha\gamma}^{set} = 0.48 \pm 0.16\,\mu\text{eV}$, by taking a typical direct ground state branching ratio of $\approx 50\,\%$ for 1^- states in ^{22}Ne into account. However, with our newly adopted $J^\pi = 0^+$ assignment the direct $0^+ \to 0^+$ ground state branching ratio becomes very small because $0^+ \to 0^+$ transitions cannot proceed via a direct γ-ray transition. Since cascade transitions bypassing the first excited 2^+ state have typically very small contributions, only a minor correction should be applied to the mea-

sured partial resonance strength from Ref. [24].

From the relative spectroscopic factor of 0.15 reported in the α-transfer study of Ref. [23], a value of $\theta_\alpha^2 = 0.64$ can be derived using the procedure outlined above in Sect. III A. Together with the result from the α-capture measurement quoted above, we adopt an average value of $\theta_\alpha^2 = 0.46$ for this state. The resulting resonance strength in the $^{18}\text{Ne}(\alpha,p)^{21}\text{Na}$ reaction amounts to $\omega\gamma_{\alpha p} = 65\,\text{eV}$, with an estimated uncertainty of a factor of two.

IV. MONTE CARLO-BASED REACTION RATES

The $^{18}\text{Ne}(\alpha,p)^{21}\text{Na}$ reaction rate can be calculated directly from Eq. (1) by adopting resonance energies, E, from Ref. [3] and resonance strengths, $\omega\gamma_{\alpha p}$, from Table I. More than 30 resonances enter into the sum of Eq. (1). Thus the uncertainties of more than 60 parameters (resonance energies and resonance strengths) must be considered simultaneously for the total reaction rate. Additional uncertainties arise for some resonances from ambiguous spin-parity assignments. The latter uncertainties could not reliably be taken into account in previous work [3, 4].

Here we present for the first time an evaluation of the experimental $^{18}\text{Ne}(\alpha,p)^{21}\text{Na}$ reaction rate using the Monte Carlo method introduced by Refs. [10–13]. The method of [10–13] had to be extended for a proper treatment of uncertain J^π assignments which will be discussed in detail later. Briefly summarizing [10–13], for each input parameter (i.e., in the present case for each resonance energy, E, and each resonance strength, $\omega\gamma$) a probability density function is obtained, based on the experimental mean value and the uncertainty. We assumed a Gaussian probability density function for resonance energies, and a lognormal one for resonance strengths. For those resonances with unknown strengths, α-particle partial widths were sampled according to a Porter-Thomas distribution with an absolute upper limit determined from Eq. (4). These choices are justified in Refs. [10, 26]. These input probability densities are sampled many times and each time a reaction rate sample is obtained. The combined ensemble of samples can then be used to define statistically meaningful recommended reaction rates and uncertainties that correspond to a desired coverage probability. In this work, we adopt the 50th percentile of the cumulative rate distribution as the recommended rate, $N_A\langle\sigma v\rangle_{\text{rec}}$, and the 16th and 84th percentiles as the low rate, $N_A\langle\sigma v\rangle_{\text{low}}$, and the high rate, $N_A\langle\sigma v\rangle_{\text{high}}$, respectively (for a coverage probability of 68%). The above percentiles are taken in analogy to the 1σ uncertainty of the usual Gaussian distribution. It is also possible to provide a 95% coverage interval, analog to the 2σ uncertainty. However, it should be kept in mind that the lognormal distribution of the resonance strengths leads to an approximately lognormal distribution of the reaction rate, and thus the low and the high rate are not

symmetric around the recommended median rate. Some numrical values will be given later for the temperature of $T_9 = 1$. Further technical details and probability density distributions for the reaction rate $N_A\langle\sigma v\rangle$ are given in [34].

In a first calculation all spins and parities J^π in Table I were used. However, because some J^π assignments are only tentative, this calculation underestimates the uncertainty of the reaction rate $N_A\langle\sigma v\rangle$. Therefore, in a second calculation we took into account these uncertain J^π assignments, and an improved estimate of the resulting uncertainty of $N_A\langle\sigma v\rangle$ could be derived.

The result of the initial Monte-Carlo calculation with the fixed J^π assignments in Table I is shown in Fig. 3. It is close to the previous recommendation of 0.55 $N_A\langle\sigma v\rangle_{\rm ref}$ [4] for temperatures $1 \lesssim T_9 \lesssim 2$ and slightly lower in the low temperature range of $0.5 \lesssim T_9 \lesssim 1$. The lower rate results from the unnatural parity of the state at $E^* = 8.385\,{\rm MeV}$ and the smaller reduced widths θ_α^2 of several category D states around $E^* = 8.5 - 9\,{\rm MeV}$.
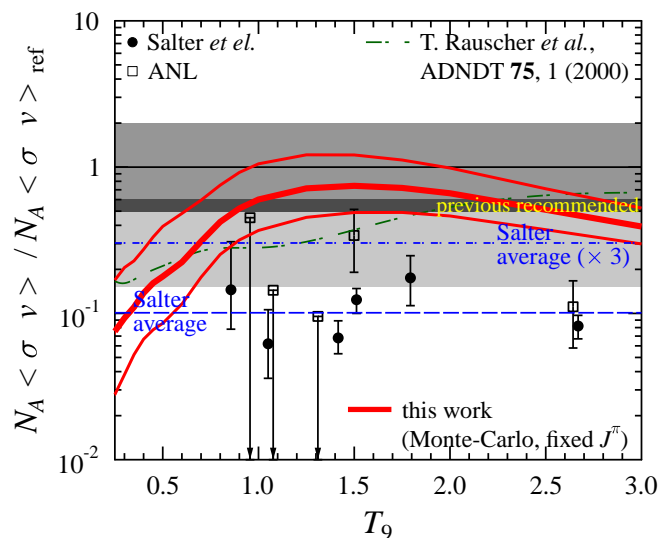

FIG. 3. (Color online) Ratio between the reaction rate $N_A\langle\sigma v\rangle$ from different studies normalized to the reference rate $N_A\langle\sigma v\rangle_{\rm ref}$ from [4]. The conversion of the experimental data from the reverse $^{21}{\rm Na}(p,\alpha)^{18}{\rm Ne}$ reaction to the shown $N_A\langle\sigma v\rangle$ data points is explained in [4]. The line "Salter average" marks the average result from [7] (ground state contribution only), "Salter average ($\times 3$)" corrects for contributions of excited states (for details see [4, 7]). The new result (thick red line) and its uncertainties (thin red lines) are close to the previous recommendation which is 0.55 $N_A\langle\sigma v\rangle_{\rm ref}$ [4] (dark grey bar). A theoretical prediction in the statistical model is also shown (green dash-dotted) [33]. Further discussion see text.

The method outlined in [10–13] assumed an unique J^π assignment for the random sampling over nuclear physics input parameters (resonance energies, strengths, S-factors, partial widths, etc.). Here we extend the method by allowing for ambiguous J^π assignments. If the J^π value of a given level is not known unambiguously, we randomly sample over possible J^π according to

a discrete probability density. The probabilities assigned to each J^π value have to be chosen according to the best knowledge available (guided by experimental or theoretical information). If J^π has been restricted to a range, and no other information is available, then the probabilities for each J^π value should be the same.

For the $^{18}{\rm Ne}(\alpha,p)^{21}{\rm Na}$ reaction under study, the J^π assignments of Table I were varied in the following way. The tentative assignment in Table I was assumed with a 50 % probability. (Arguments for these tentative assignments are mainly taken from [3].) The remaining 50 % were distributed uniformly among other possible assignments, e.g. taken from Table II of [19] ("χ^2 values for possible l transfers") or from uncertain assignments in the mirror nucleus [23]. If there is no restriction on J^π from resonant elastic scattering or from α transfer reactions, the remaining 50 % were distributed uniformly among all natural parity states from 0^+ to 4^+. The chosen values are listed in Table II. In cases with a well-defined J^π assignment in the $^{22}{\rm Ne}$ mirror nucleus (e.g., from α-transfer in [23]), no variation of J^π in $^{22}{\rm Mg}$ was allowed, and the adopted J^π of Table I was used. This is justified by a cancellation effect which will be discussed later (see Sect. V B).

Although carefully chosen, it is obvious that the above assumptions on the chosen probabilities of J^π are somewhat arbitrary. Nevertheless, the derived $N_A\langle\sigma v\rangle$ and in particular its uncertainty should be more realistic than all previous estimates where in most cases only fixed J^π assignments were considered (i.e., neglecting any uncertain J^π). As the other extreme, a fully random J^π assignment was used in [3] to estimate an upper limit of the uncertainty of $N_A\langle\sigma v\rangle$ from the J^π assignments; here an uncertainty of about a factor of 10 was found.

Using the larger parameter space with variable J^π assignments from Table II in our Monte-Carlo sampling, we find that the reaction rate $N_A\langle\sigma v\rangle$ remained within about 20 % of the result with fixed J^π assignments. The reason for these minor changes is that variable J^π assignments have to be taken into account mainly for category D states (without spectroscopic information) which have relatively small resonance strengths because of their small reduced widths θ_α^2. The result is shown in Fig. 4, and numerical values are listed in Table III. The overall uncertainty is slightly above a factor of two at low temperatures ($T_9 \approx 0.5$), and reduces to about a factor of 1.5 for $1 \lesssim T_9 \lesssim 3$. The uncertainty in the total rate can be smaller than the uncertainty in individual resonance parameters because the rate calculation averages over the contributing resonances. For simple use in astrophysical calculations, a fit to the reaction rate $N_A\langle\sigma v\rangle$ of the $^{18}{\rm Ne}(\alpha,p)^{21}{\rm Na}$ reaction is provided in the Appendix A.

For interpretation of the rate $N_A\langle\sigma v\rangle$ and the given uncertainties in Table III, we discuss in detail the result for the temperature $T_9 = 1.0$. All $N_A\langle\sigma v\rangle$ in the following discussion are given in $10^{-3}\,{\rm cm}^3\,{\rm s}^{-1}\,{\rm mol}^{-1}$ (without explicitly repeating this unit). Our recommended result is 60.9 which is the median of the 10,000 Monte-Carlo sam-

TABLE II. Variable J^π assignments for the improved estimate of the uncertainty of the reaction rate $N_A\langle\sigma v\rangle$ of the ^{18}Ne$(\alpha,p)^{21}$Na reaction. A probability of $p = 1/2$ is assumed for the J^π assignments in Table I (marked in bold). The remaining 50 % are distributed among other possible J^π. The given numbers $p(J^\pi)$ are used as discrete probability densities for Monte-Carlo sampling of the reaction rate $N_A\langle\sigma v\rangle$. Further details see text.

$E^*(^{22}$Mg$)$ (MeV)	E (MeV)	J^π	$p(J^\pi)$
9.318	1.176	0^+	$1/8$
		1^-	$1/8$
		$\mathbf{2^+}$	$\mathbf{1/2}$
		3^-	$1/8$
		4^+	$1/8$
9.482	1.340	2^+	$1/4$
		$\mathbf{3^-}$	$\mathbf{3/4}$
9.752	1.610	1^-	$1/2$
		$\mathbf{2^+}$	$\mathbf{1/2}$
9.860	1.718	$\mathbf{0^+}$	$\mathbf{1/2}$
		1^-	$1/4$
		2^+	$1/4$
10.085	1.943	0^+	$1/4$
		1^-	$1/4$
		$\mathbf{2^+}$	$\mathbf{1/2}$
10.651	2.509	0^+	$1/8$
		1^-	$1/8$
		2^+	$1/8$
		$\mathbf{3^-}$	$\mathbf{1/2}$
		4^+	$1/8$
10.768	2.626	0^+	$1/8$
		1^-	$1/8$
		$\mathbf{2^+}$	$\mathbf{1/2}$
		3^-	$1/8$
		4^+	$1/8$
10.873	2.731	$\mathbf{0^+}$	$\mathbf{1/2}$
		1^-	$1/8$
		2^+	$1/8$
		3^-	$1/8$
		4^+	$1/8$
11.001	2.859	0^+	$1/8$
		1^-	$1/8$
		2^+	$1/8$
		3^-	$1/8$
		$\mathbf{4^+}$	$\mathbf{1/2}$
11.315	3.173	0^+	$1/8$
		1^-	$1/8$
		2^+	$1/8$
		3^-	$1/8$
		$\mathbf{4^+}$	$\mathbf{1/2}$
11.595	3.453	3^-	$1/3$
		$\mathbf{4^+}$	$\mathbf{2/3}$

FIG. 4. (Color online) Same as Fig. 3, but with the additional uncertainty from the spin assignments J^π in Table II. The new reaction rate $N_A\langle\sigma v\rangle$ using variable J^π assignments is slightly higher than the first calculation with fixed J^π in Fig. 3 but remains close to the previous recommendation which is $0.55\ N_A\langle\sigma v\rangle_{\mathrm{ref}}$ [4] (dark grey bar).

tion of the calculated reaction rates. A wider uncertainty band with 95 % coverage can be taken from the 2.3rd and 97.7th percentile of the Monte-Carlo samples, leading to a wider range for $N_A\langle\sigma v\rangle$ between 23 and 184.

The Monte Carlo method also provides the fractional contributions of individual resonances to the total rate. On a sample-by-sample basis, the fractional contributions of all resonances can be computed to obtain an ensemble of contributions over the full Monte Carlo calculation. Similar to the definition of low and high reaction rates via percentiles, for these ensembles of fractional contributions low and high contributions are given at the 16th and 84th percentiles. This method ensures that individual contributions and their uncertainties do not exceed unity or become negative. These contributions are displayed in Fig. 5. It is apparent that the total rate is dominated by few strong resonances. At typical break-out temperatures slightly below $T_9 = 1$, the 1^- resonance at $938\,\mathrm{keV}$ (shown in red) contributes more than 50 % to the total rate. At slightly higher temperatures around $T_9 = 1 - 2$, the 1^- resonance at $1401\,\mathrm{keV}$, the broad 0^+ resonance at $1567\,\mathrm{keV}$, and at moderate extent the $(1^-, 2^+)$ resonance at $1610\,\mathrm{keV}$ dominate the total rate.

ples which were calculated. The 16th percentile gives the recommended lower rate of 37.2; i.e., 1,600 of the 10,000 Monte-Carlo samples provided a rate below 37.2. Similar to the recommended lower rate, the recommended upper rate of 102 is defined at 84th percentile. The uncertainty of the new recommended rate of 60.9 is a factor of 1.67, covering 68 % of the probability density distribution and reflecting the approximately lognormal distribu-
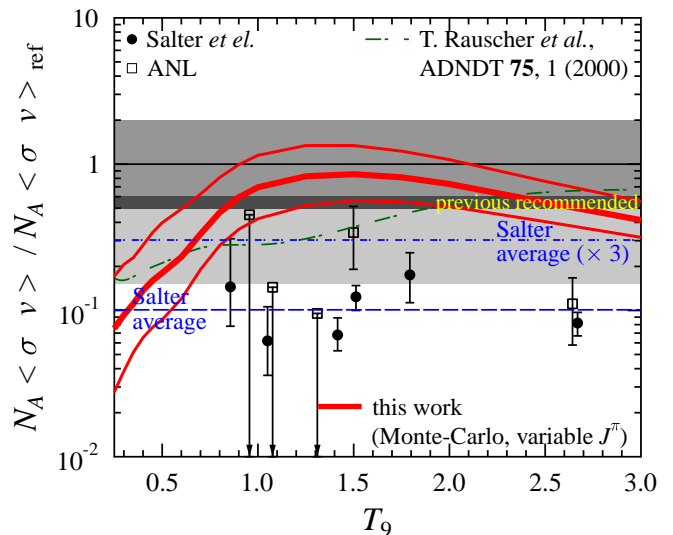
V. DISCUSSION

A. Comparison to previous work

Our recommended rate is slightly higher than the previous rate [4] at intermediate temperatures ($T_9 = 1 - 2$),

TABLE III. Recommended reaction rate $N_A\langle\sigma v\rangle_{\rm rec}$ of the ^{18}Ne(α,p)^{21}Na reaction (in cm^3 s^{-1} mol^{-1}) from Monte-Carlo sampling. The underlying input parameters for the Monte-Carlo approach are based on experimental information from various sources (for details see text).

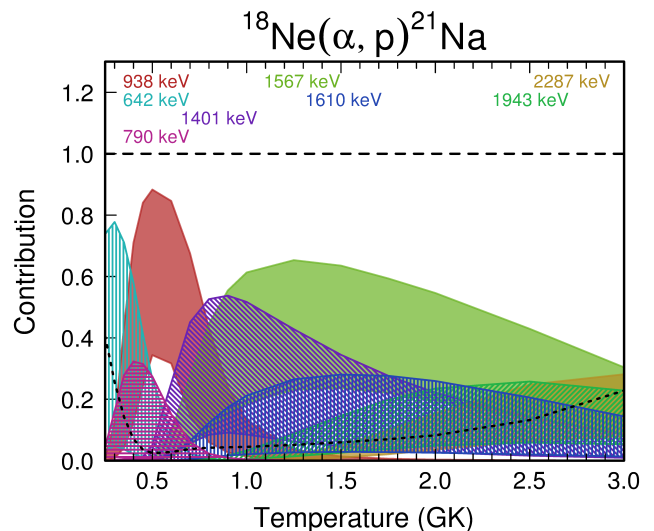| T_9	low	rec	high
0.1	2.00×10^{-27}	5.94×10^{-27}	1.76×10^{-26}
0.2	4.36×10^{-17}	1.12×10^{-16}	2.74×10^{-16}
0.3	2.04×10^{-12}	5.00×10^{-12}	1.11×10^{-11}
0.4	1.33×10^{-09}	2.78×10^{-09}	5.60×10^{-09}
0.5	1.13×10^{-07}	2.35×10^{-07}	5.12×10^{-07}
0.6	3.69×10^{-06}	7.09×10^{-06}	1.51×10^{-05}
0.7	7.10×10^{-05}	1.25×10^{-04}	2.36×10^{-04}
0.8	8.54×10^{-04}	1.44×10^{-03}	2.49×10^{-03}
0.9	6.67×10^{-03}	1.11×10^{-02}	1.87×10^{-02}
1.0	3.72×10^{-02}	6.09×10^{-02}	1.02×10^{-01}
1.1	1.57×10^{-01}	2.54×10^{-01}	4.22×10^{-01}
1.2	5.28×10^{-01}	8.48×10^{-01}	$1.39\times10^{+00}$
1.3	$1.49\times10^{+00}$	$2.37\times10^{+00}$	$3.86\times10^{+00}$
1.4	$3.70\times10^{+00}$	$5.76\times10^{+00}$	$9.23\times10^{+00}$
1.5	$8.16\times10^{+00}$	$1.25\times10^{+01}$	$1.97\times10^{+01}$
1.6	$1.64\times10^{+01}$	$2.47\times10^{+01}$	$3.84\times10^{+01}$
1.7	$3.06\times10^{+01}$	$4.54\times10^{+01}$	$6.94\times10^{+01}$
1.8	$5.34\times10^{+01}$	$7.83\times10^{+01}$	$1.18\times10^{+02}$
1.9	$8.84\times10^{+01}$	$1.28\times10^{+02}$	$1.89\times10^{+02}$
2.0	$1.40\times10^{+02}$	$2.01\times10^{+02}$	$2.93\times10^{+02}$
2.1	$2.13\times10^{+02}$	$3.03\times10^{+02}$	$4.37\times10^{+02}$
2.2	$3.13\times10^{+02}$	$4.42\times10^{+02}$	$6.30\times10^{+02}$
2.3	$4.49\times10^{+02}$	$6.27\times10^{+02}$	$8.84\times10^{+02}$
2.4	$6.31\times10^{+02}$	$8.71\times10^{+02}$	$1.21\times10^{+03}$
2.5	$8.69\times10^{+02}$	$1.19\times10^{+03}$	$1.64\times10^{+03}$
2.6	$1.17\times10^{+03}$	$1.59\times10^{+03}$	$2.18\times10^{+03}$
2.7	$1.57\times10^{+03}$	$2.10\times10^{+03}$	$2.86\times10^{+03}$
2.8	$2.06\times10^{+03}$	$2.75\times10^{+03}$	$3.71\times10^{+03}$
2.9	$2.69\times10^{+03}$	$3.55\times10^{+03}$	$4.75\times10^{+03}$
3.0	$3.44\times10^{+03}$	$4.55\times10^{+03}$	$6.06\times10^{+03}$

FIG. 5. (Color online) Contributions of individual resonances to the reaction rate $N_A\langle\sigma v\rangle$. Only few resonances contribute significantly to $N_A\langle\sigma v\rangle$ in the most important temperature range around $T_9 = 0.5-2$. The black dashed line corresponds to the total contribution of all other resonances not explicitly displayed in the plot.

firm for most levels earlier tentative assignments adopted in Refs. [3, 4]. New spin-parity assignments have been made only for a few states, and in particular the resonance at 243 keV has been excluded because of its un-natural parity. This leads to slightly reduced $N_A\langle\sigma v\rangle$ at low temperatures in [6] compared to Ref. [4].

B. An interesting cancellation effect

The remaining influence of uncertain mirror assignments on $N_A\langle\sigma v\rangle$ is surprisingly small. This is mainly based on an interesting cancellation effect. The following discussion extends a similar idea which was already presented by Iliadis *et al.* [35] for a fictitious resonance in the ^{35}Ar(p,γ)^{36}K reaction. Let us consider here the 0^+ resonance at 1567 keV as an example.

Matic *et al.* [3] have assigned the 0^+ state at $E^* = 10052$ keV in ^{22}Ne as the mirror state. For this mirror state a large reduced width of $\theta_\alpha^2 = 0.46$ has been found in the ^{18}O(α,γ)^{22}Ne and ^{18}O(^{6}Li,d)^{22}Ne reactions [21–24]; thus, the α-cluster properties of this state in ^{22}Ne are well-established from experiment, and also theory suggests such a state [30–32]. Based on mirror symmetry, a state with a similar α-cluster wave function should exist also in ^{22}Mg around $E^* \approx 10$ MeV.

Let us now first assume that the mirror assignment in [3] is correct. Then this state appears as a resonance in the ^{18}Ne(α,p)^{21}Na reaction at $E = 1567$ keV with a resonance strength of $\omega\gamma = 65$ eV. It contributes to the rate with $N_A\langle\sigma v\rangle = 5.1$ cm^3 s^{-1} mol^{-1} e.g. at $T_9 = 1.5$.

Let us next consider what happens if this mirror as-

slightly lower at high temperatures ($T_9 \gg 2$), and significantly lower for very low temperatures ($T_9 < 0.5$). These differences are a direct consequence of the changes in the astrophysical S-factor (Fig. 2) that were discussed in Sec. III A.

The reaction rate of Ref. [3] is much higher than the present result because the former was obtained by using some huge strengths measured in Ref. [9] that are in contradiction to the experimental data for the reverse reaction [7, 8], as pointed out by Ref. [4].

The reaction rate of Salter *et al.* [7] is much lower than the present result since it was directly derived from the experimental reverse reaction data. As noted above, this procedure provides the ground state contribution only, which obviously must be smaller than the total reaction rate.

The reaction rate obtained in the recent study of ^{21}Na(p,p)^{21}Na resonant elastic scattering by Zhang *et al.* [6] is close to the earlier recommendation of Ref. [4]. In general, Zhang *et al.* adopt the resonance strengths from Ref. [4] because the new J^π assignments of Ref. [6] con-

signment is incorrect. If the α-strength with $\theta_\alpha^2 = 0.46$ is located about $250\,\mathrm{keV}$ lower (higher), then the resonance strength decreases (increases) by about one order of magnitude to $\omega\gamma = 6.2\,\mathrm{eV}$ ($422\,\mathrm{eV}$). Nevertheless, the changes in $N_A\langle\sigma v\rangle$ at $T_9 = 1.5$ remain within less than a factor of two with $N_A\langle\sigma v\rangle = 3.2\,\mathrm{cm^3\,s^{-1}\,mol^{-1}}$ ($4.6\,\mathrm{cm^3\,s^{-1}\,mol^{-1}}$) for the lower (higher) energy.

The explanation for this mild dependence can be read from Eq. (1). The reaction rate $N_A\langle\sigma v\rangle$ scales exponentially with the resonance energy in the factor $\exp(-11.605E/T_9)$, and it scales linearly with the resonance strength $\omega\gamma \approx (2J+1)\Gamma_\alpha = (2J+1)\,\theta_\alpha^2\,\Gamma_\alpha^{s.p.}$. However, $\Gamma_\alpha^{s.p.}$ scales exponentially with the resonance energy. Thus, for a given θ_α^2 (determined in the mirror nucleus) we find that $N_A\langle\sigma v\rangle$ is the product of an exponentially rising resonance strength and an exponentially decreasing factor $\exp(-11.605E/T_9)$ (the latter factor results from the Maxwell-Boltzmann distribution). This product shows a maximum very similar to the conventional Gamow window. For the given example this is illustrated in Fig. 6; the above discussed temperature of $T_9 = 1.5$ is shown in the middle part.
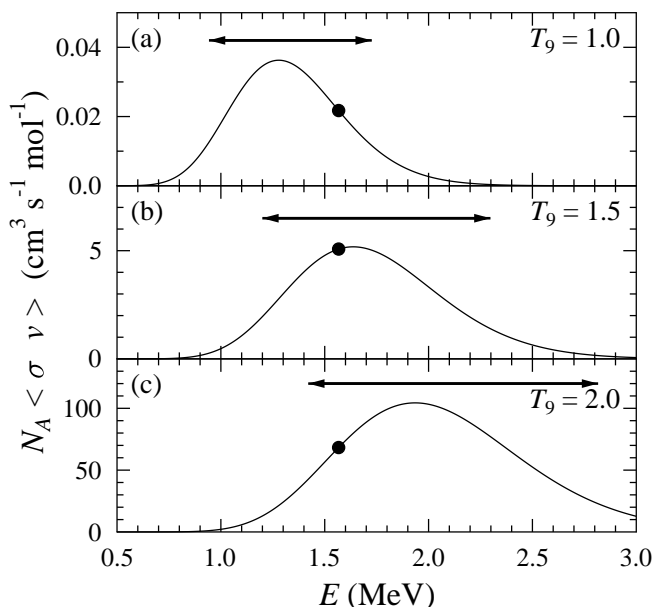

FIG. 6. Reaction rate $N_A\langle\sigma v\rangle$ for a 0^+ resonance with $\theta_\alpha^2 = 0.46$ in ^{22}Mg as a function of resonance energy E for three temperatures $T_9 = 1.0$ (a), 1.5 (b), and 2.0 (c) (from top to bottom). The data point indicates $E = 1567\,\mathrm{keV}$ which has been assigned as mirror of the 0^+ state in ^{22}Ne at $E^* = 10052\,\mathrm{keV}$. The arrows indicate the position of the usual Gamow window. For further discussion see text.

At $T_9 = 1.5$ the resonance at $1567\,\mathrm{keV}$ is located almost in the center of the usual Gamow window which is given by the most effective energy $E_0 = 0.122\,(Z_1^2 Z_2^2 A_{\mathrm{red}} T_9^2)^{1/3}\,\mathrm{MeV}$ and the $1/e$ width $\Delta = 0.237\,(Z_1^2 Z_2^2 A_{\mathrm{red}} T_9^5)^{1/6}\,\mathrm{MeV}$ (see Refs. [14, 36]). Thus, the reaction rate $N_A\langle\sigma v\rangle$ is close to its maximum for $E = 1567\,\mathrm{keV}$, and $N_A\langle\sigma v\rangle$ decreases slightly for lower and higher resonance energies E.

At lower temperatures, e.g. $T_9 = 1.0$ (Fig. 6, upper part), the most effective energy E_0 is lower, and the resonance at $E = 1567\,\mathrm{keV}$ is located on the high-energy side of the Gamow window. For $E = 1567\,\mathrm{keV}$ a reaction rate $N_A\langle\sigma v\rangle = 0.022\,\mathrm{cm^3\,s^{-1}\,mol^{-1}}$ is found. If the resonance is lowered in energy by $250\,\mathrm{keV}$, now the rate increases to $N_A\langle\sigma v\rangle = 0.036\,\mathrm{cm^3\,s^{-1}\,mol^{-1}}$ because this lower resonance energy is located in the center of the Gamow window. Increasing the resonance energy by $250\,\mathrm{keV}$ leads to a further reduced rate of $N_A\langle\sigma v\rangle = 0.008\,\mathrm{cm^3\,s^{-1}\,mol^{-1}}$.

At higher temperatures, e.g. $T_9 = 2.0$ (Fig. 6, lower part), the most effective energy E_0 is higher, and now $E = 1567\,\mathrm{keV}$ leads to $N_A\langle\sigma v\rangle = 68\,\mathrm{cm^3\,s^{-1}\,mol^{-1}}$. For the resonance with $250\,\mathrm{keV}$ lowered energy the rate $N_A\langle\sigma v\rangle = 27\,\mathrm{cm^3\,s^{-1}\,mol^{-1}}$ is lower, and for the resonance with $250\,\mathrm{keV}$ increased energy the rate $N_A\langle\sigma v\rangle = 100\,\mathrm{cm^3\,s^{-1}\,mol^{-1}}$ is higher.

In conclusion this means that the experimentally confirmed α-cluster state in ^{22}Ne at $E^* = 10052\,\mathrm{keV}$ with $\theta_\alpha^2 = 0.46$ leads to a relatively well-constrained reaction rate $N_A\langle\sigma v\rangle$ of the ^{18}Ne$(\alpha,p)^{21}$Na reaction for temperatures $T_9 = 1 - 2$ as long as (i) the principle of mirror symmetry is accepted and (ii) the mirror state in ^{22}Mg is located anywhere within a $500\,\mathrm{keV}$ broad window around the currently accepted mirror assignment at $E^* = 9709\,\mathrm{keV}$ ($E = 1567\,\mathrm{keV}$).

The above argument can be generalized. It is very helpful to determine reduced widths θ_α^2 (e.g. from the mirror system) for resonances which are located in the classical Gamow window because the reduced width θ_α^2 essentially constrains the reaction rate $N_A\langle\sigma v\rangle$ even in cases when the mirror assignment is unclear or only tentative.

VI. SUMMARY AND CONCLUSIONS

The stellar reaction rate $N_A\langle\sigma v\rangle$ of the ^{18}Ne$(\alpha,p)^{21}$Na reaction is composed of the contributions of 32 resonances. The Monte-Carlo method has been applied to calculate $N_A\langle\sigma v\rangle$ from experimental resonance energies [3] and resonance strengths which were calculated using reduced widths θ_α^2 either from the mirror nucleus [21–25] or from a Porter-Thomas distribution found in a recent systematic study [26]. Furthermore, uncertainties from tentative J^π assignments were taken into account by Monte-Carlo sampling of discrete probability distributions. The recommended result for $N_A\langle\sigma v\rangle$ is close to previous recommendations [4, 6]. Nevertheless, there is significant progress compared to these previous recommendations: In [4, 6] the recommended rate was composed as a compromise between a relatively high $N_A\langle\sigma v\rangle$ from resonance energies and calculated resonance strengths and a relatively low $N_A\langle\sigma v\rangle$ from the reverse reaction data. Now the newly determined resonance strengths are somewhat lower, thus bringing both

approaches for the determination of $N_A\langle\sigma v\rangle$ in better agreement and increasing the reliability of the result.

In addition, the Monte-Carlo formalism allows an improved determination of uncertainties which takes into account the uncertainties of all ingredients in a consistent way. It turns out that the uncertainty of $N_A\langle\sigma v\rangle$ is essentially given by the uncertainties of the resonance strengths whereas the resonance energies of [3] are sufficiently precise. The uncertainties of the resonance strengths were estimated according to the available information on the reduced α-width θ_α^2 in the ^{22}Ne mirror nucleus. As final result we find that $N_A\langle\sigma v\rangle$ (given as the median of the Monte-Carlo sampling) has an uncertainty of less than a factor of two (given as the 68 % coverage probability of the Monte-Carlo sampling) in the astrophysically relevant temperature range.

Under typical astrophysical conditions of X-ray bursters (density $\rho \approx 10^6$ g/cm^3 and α mass fraction $Y_\alpha \approx 0.27$) we find that the rate of the ^{18}Ne$(\alpha,p)^{21}$Na reaction exceeds the β^+-decay rate of ^{18}Ne at $T_9 = 0.60 \pm 0.02$; i.e., the break-out temperature is very well constrained by the present work. At this break-out temperature $N_A\langle\sigma v\rangle$ is mainly determined by the resonance at 938 keV with its newly confirmed $J^\pi = 1^-$ assignment [6].

[1] H. Schatz and K. E. Rehm, Nucl. Phys. **A777**, 601 (2006).
[2] A. Parikh, J. José, F. Moreno and C. Iliadis, Astrophys. J. Suppl. **178**, 110 (2008).
[3] A. Matic *et al.*, Phys. Rev. C **80**, 055804 (2009).
[4] P. Mohr and A. Matic, Phys. Rev. C **87**, 035801 (2013).
[5] J. J. He *et al.*, Phys. Rev. C **88**, 012801(R) (2013).
[6] L. Y. Zhang *et al.*, Phys. Rev. C **89**, 015804 (2014).
[7] P. J. C. Salter *et al.*, Phys. Rev. Lett. **108**, 242701 (2012).
[8] S. Sinha *et al.*, ANL Annual Report 2005, p.6-7.
[9] D. Groombridge *et al.*, Phys. Rev. C **66**, 055802 (2002).
[10] R. Longland, C. Iliadis, A. E. Champagne, J. R. Newton, C. Ugalde, A. Coc, R. Fitzgerald, Nucl. Phys. **A841**, 1 (2010).
[11] C. Iliadis, R. Longland, A. E. Champagne, A. Coc, R. Fitzgerald, Nucl. Phys. **A841**, 31 (2010).
[12] C. Iliadis, R. Longland, A. E. Champagne, A. Coc, Nucl. Phys. **A841**, 251 (2010).
[13] C. Iliadis, R. Longland, A. E. Champagne, A. Coc, Nucl. Phys. **A841**, 323 (2010).
[14] C. Iliadis, Nuclear Physics of Stars, Wiley-VCH, Weinheim, Germany (2007).
[15] *http://www-nds.iaea.org/amdc/*; G. Audi, F. G. Kondev, M. Wang, B. Pfeiffer, X. Sun, J. Blachot, M. MacCormick, Chin. Phys. C **36**, 1157 (2012); G. Audi, M. Wang, A. H. Wapstra, F. G. Kondev, M. MacCormick, X. Xu, B. Pfeiffer, Chin. Phys. C **36**, 1287 (2012); M. Wang, G. Audi, A. H. Wapstra, F. G. Kondev, M. MacCormick, X.Xu, B. Pfeiffer, Chin. Phys. C **36**, 1603 (2012).
[16] A. A. Chen, R. Lewis, K. B. Swartz, D. W. Visser, P. D. Parker, Phys. Rev. C **63**, 065807 (2001).
[17] J. A. Caggiano *et al.*, Phys. Rev. C **66**, 015804 (2002).
[18] G. P. A. Berg *et al.*, Nucl. Phys. **A718**, 608 (2003).
[19] K. Y. Chae *et al.*, Phys. Rev. C **79**, 055804 (2009).
[20] F. de Oliveira *et al.*, Phys. Rev. C **55**, 3149 (1997).
[21] H. P. Trautvetter, M. Wiescher, K.-U. Kettner, C. Rolfs, J. W. Hammer, Nucl. Phys. **A297**, 489 (1978).
[22] R. B. Vogelaar, T. R. Wang, S. E. Kellogg, R. W. Kavanagh, Phys. Rev. C **42**, 753 (1990).
[23] U. Giesen, C. P. Browne, J. Görres, J. G. Ross, M. Wiescher, R. E. Azuma, J. D. King, J. B. Vise, M. Buckby, Nucl. Phys. **A567**, 146 (1994).

[24] S. Dababneh, M. Heil, F. Käppeler, J. Görres, M. Wiescher, R. Reifarth, H. Leiste, Phys. Rev. C **68**, 025801 (2003).
[25] V. Z. Goldberg *et al.*, Phys. Rev. C **69**, 024602 (2004).
[26] I. Pogrebnyak, C. Howard, C. Iliadis, R. Longland, G. E. Mitchell, Phys. Rev. C **88**, 015808 (2013).
[27] Data base *ENDSF*, available online at *www.nndc.bnl.gov/ensdf*.
[28] X. K. Maruyama, R. A. Lindgren, W. L. Bendel, E. C. Jones, Jr., L. W. Fagg, Phys. Rev. C **10**, 2257 (1974).
[29] U. E. P. Berg and K. Wienhard, Nucl. Phys. **A318**, 453 (1979).
[30] G. Lévai, Phys. Rev. C **88**, 014328 (2013).
[31] M. Kimura, Phys. Rev. C **75**, 034312 (2007).
[32] P. Descouvemont, Phys. Rev. C **38**, 2397 (1988).
[33] T. Rauscher and F.-K. Thielemann, At. Data Nucl. Data Tables **75**, 1 (2000).
[34] P. Mohr, R. Longland, C. Iliadis, Proc. *Nuclei in the Cosmos XIII*, Debrecen, Hungary, Proceedings of Science, PoS(NIC-XIII)036, submitted.
[35] C. Iliadis, P. M. Endt, N. Prantzos, W. J. Thompson, Astroph. J. **524**, 434 (1999).
[36] C. E. Rolfs and W. S. Rodney, Cauldrons in the Cosmos, The University of Chicago Press, Chicago, USA (1988).

Appendix A: Fit of the reaction rate $N_A\langle\sigma v\rangle$

The recommended reaction rate $N_A\langle\sigma v\rangle_{\rm rec}$ is fitted by the usual expression, see e.g. [33], Eq. (16):

$$\frac{N_A <\sigma v>}{\rm cm^3 s^{-1} mol^{-1}} = \exp\left(a_0 + a_1 T_9^{-1} + a_2 T_9^{-1/3} + a_3 T_9^{1/3} + a_4 T_9 + a_5 T_9^{5/3} + a_6 \ln T_9\right) \quad (A1)$$

The a_i parameters are listed in Table IV. The deviation of the fitted rate is always below 12 % over the full temperature range $0.25 \leq T_9 \leq 3$ and typically far below 5 % in the most relevant range $1 \leq T_9 \leq 2$; but the fit should not be used below $T_9 = 0.2$ or above $T_9 = 3.5$.

TABLE IV. Fit parameters a_i of the recommended reaction rate $N_A \langle \sigma v \rangle_{\mathrm{rec}}$ from Eq. (A1). The parametrization is valid for the full temperature range $0.25 \leq T_9 \leq 3$ with a deviation of less than $12\,\%$. The fit formula in Eq. (A1) should not be used below $T_9 = 0.2$ or above $T_9 = 3.5$.

a_0	a_1	a_2	a_3	a_4	a_5	a_6
590.68	-52.89	1916.23	-2586.60	136.60	-6.86	1338.35